Bioorganic & Medicinal Chemistry xxx (2014) xxx–xxx

Contents lists available at ScienceDirect

Bioorganic & Medicinal Chemistry

journal homepage: www.elsevier.com/locate/bmc

Identification of novel thiadiazoloacrylamide analogues as inhibitors of dengue-2 virus NS2B/NS3 protease

Hailong Liu [a,b,†], Ruoming Wu [c,†], Yanyan Sun [c], Yan Ye [a], Jing Chen [a,*], Xiaomin Luo [a], Xu Shen [a], Hong Liu [a,*]

[a] Key Laboratory of Receptor Research, Shanghai Institute of Materia Medica, Chinese Academy of Sciences, Shanghai 201203, China
[b] School of Pharmacy, China Pharmaceutical University, Jiangsu, Nanjing 210009, China
[c] School of Pharmacy, East China University of Science and Technology, Shanghai 200237, China

ARTICLE INFO

Article history:
Received 12 August 2014
Revised 24 September 2014
Accepted 26 September 2014
Available online xxxx

Keywords:
Thiadiazo
Dengue virus
NS2B/NS3

ABSTRACT

Dengue virus is endemic throughout tropical and subtropical regions, and cause severe epidemic diseases. The NS2B/NS3 protease is a promising drug target for dengue virus. Herein, we report the discovery and modification of a novel class of thiadiazoloacrylamide derivatives with potent inhibitory activity against the NS2B/NS3 protease. Thiadiazolopyrimidinone **1** was firstly determined as a new chemical structure against NS2B/NS3 from a commercial compound library. Then, we sought to identify similar compounds with the thiadiazoloacrylamide core that would exhibit better activity. A series of analogues were synthesized and fourteen of them were identified with strong inhibitory activities, in which the nitrile group in the linker part was discovered as an essential group for the inhibitory activity. The best of these (**8b**) demonstrated an IC_{50} at 2.24 μM based on in vitro DENV2 NS2B-NS3pro assays.

1. Introduction

Dengue virus (DENV), together with other serious pathogens such as West Nile viruses (WNVs), Yellow *Feverviruses* (YFVs) and Japanese encephalitis viruses (JEVs), belong to the *Flaviviridae* family. DENV infection causes severe epidemic disease ranging from the mild dengue fever (DF) to the life-threatening dengue hemorrhagic fever (DHF) and dengue shock syndrome (DSS).[1] The U.S. Center for Disease Control and Prevention estimates that 2.5 billion people worldwide are at risk of DENV infection, especially in tropical and subtropical regions. Approximately 500,000 individuals cases develop DHF and DSS, with ~25,000 fatalities every year.[2] There are four distinct serotypes of dengue (DENV 1–4), each of which can cause dengue disease, but DEN2 being the most prevalent. It has been suggested that subsequent infection by different serotypes enhances the likelihood of developing more serious forms of Dengue such as DHF and DSS,[3,4] making vaccine studies more difficult to perform. To date, there is no approved vaccine or targeted drug therapy to combat this disease. Therefore, there is an urgent need for efforts to develop effective anti-dengue drugs.

Dengue virus contain a ~11 kb positive-strand RNA genome that is transcribed as a single polyprotein arranged in order NH_2-C-prM-E-NS1-NS2A-NS2B-NS3-NS4A-NS4B-NS5-COOH.[5] Subsequently, the polyprotein precursor is cleaved by both host proteases and the viral protease complex NS2B/NS3 to generate three structural proteins and seven nonstructural proteins, which are required for viral replication.[6] The N-terminal region of the nonstructural protein 3 (NS3) is a trypsin-like protease with a serine protease catalytic triad (His51, Asp75 and Ser135).[7,8] To exert the full protease activity of NS3pro, the NS2B must be presence acting as a cofactor.[9] There is a precedent for the therapeutic exploitation of protease inhibition in the treatment of HIV and hepatitis C infection, and given the indispensable role of the NS2B/NS3 protease complex in DENY replication, it serves as an ideal target for anti-dengue virus drug development.

Recently, intensive efforts have been made to find DENV NS2B/NS3 protease inhibitors. Candidates identified to date have included peptidomimetics with electrophilic warheads such as aldehydes,[10–12] ketones,[13] cyclopetide,[14,15] retro peptide-hybrids,[16] and non-petidyl agents such as anthracene-based,[17] aminobenzamides,[18] arylcyanoacrylamides,[19] benz(*d*)isothiazol-3(2H)-one derivatives,[20] 1,2-benzisothiazol-3(2H)-one derivatives.[21] Computational approaches have also been made to drug discovery in this field.[22,23] However, most of the antiviral agents reported to date

* Corresponding authors. Tel./fax: +86 21 50807042.
E-mail addresses: jingchen@simm.ac.cn (J. Chen), hliu@mail.shcnc.ac.cn (H. Liu).
† These two authors contributed equally to this work.

http://dx.doi.org/10.1016/j.bmc.2014.09.057
0968-0896/

have manifest only moderate activity, and novel inhibitors with good activity are still needed.

In this study, we present a detailed report of the synthesis of novel thiadiazoloacrylamide derivatives as potential inhibitors of the DENV2 NS2B/NS3 protease, along with biochemical and structure–activity relationship (SAR) studies.

2. Chemistry

Our work was initiated with a high-throughput screening of a commercial compound library containing ~7000 compounds and identified the thiadiazolopyrimidinone **1** as a potential NS2B/NS3 protease inhibitor. This compound (**1**, Fig. 1) was commercially obtained and exhibited inhibitory activity against DENV2 NS2B/NS3 protease with an IC_{50} value of 6.09 μM.

We aimed to undertake a study of structure–activity relationships for compound **1**. However, in the synthesis of this compound (Scheme 1), we found that we can only obtain the transamidation product **7b** rather than the desired cyclization product **1** using the previously reported methods.[24,25] This result was confirmed from the IR spectrum of the reaction product, in which a characteristic nitrile stretch was found in the region 2260–2220 cm^{-1}. We then tested the activity of thiadiazoloacrylamide compound **7b** using in vitro DENV2 NS2B/NS3 pro assays. To our delight, this product exhibited a better inhibitory activity than compound **1**, with IC_{50} value of 4.44 μM. As the thiadiazoloacrylamide **7b** has a better molecular flexibility than the screening compound **1**, making it closer to a drug-like structure, we decided to use **7b** as the benchmark compound for further study.

The synthesis of thiadiazoloacrylamide analogues **7a–i** and **8a–e** reported in this study are summarized in Scheme 2. The amino thiadiazoles **4a–i** were readily prepared from cyclodehydration between thiosemicarbazide **2** and trifluoroacetic anhydride[26] (for **4a**) or alkylation of amino thiadiazoles **3** under base conditions[27] (for **4b–i**). Another fragments **6a–f** were synthesized via condensation between different N-protected indolaldehydes **5a–f** with ethyl cyanacetate. Treatment with the two building blocks (**4a–i** and **5a–f**) in a refluxing MeONa/MeOH mixture then yielded the corresponding thiadiazoloacetamides **7a–i** and **8a–e**.

To study the role of the linker component of in the thiadiazoloacrylamides in determining the biological activity, another chemical modification was performed; synthetic routes leading to compounds **12a–b** are illustrated in the synthetic Scheme 3. The starting intermediate **4a** was coupled with acryl chlorides **9**, followed by dehydration with N-protected indolaldehyde **5** to form thiadiazoloacrylamide **11**. The target product **12a** was obtained after decarboxylation of compound **11**. Subsequently, it was hydrogenated to yield compound **12b**.

3. Biochemistry

The in vitro protease inhibition assay was used to screen the lead compound and evaluate the analogues as previously described.[28] In this assay, *aprotinin* acted as a positive control and exhibited the significant inhibitory effect against DENV2 NS2B/NS3pro. The results are summarized in Figures 2 and 3 and Tables 1 and 2. Binding affinity assay was conducted to confirm the results of the molecular modeling and the protease inhibition assay. The results are listed in Figure 5.

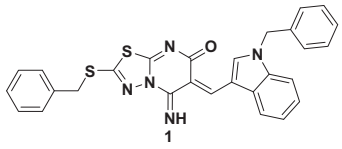

1

Figure 1. The structure of hit compound **1**.

4. Results and discussion

A series of structurally-diverse thiadiazoloacetamides were readily obtained as shown in Schemes 1 and 2, and their activities against DENV2 NS2B/NS3 protease were investigated. The structural modification of lead compound **1** was based on two main considerations: (a) it was envisaged that the thiadiazoloacetamide core would interact with the protease through multiple hydrogen bonds, essential for its inhibitory activity. Thus the thiadiazoloacetamide core was retained. (b) Based on previously reported molecular modelling studies,[15,18–20] it was hypothesized that the two aromatic rings linked by the thiadiazoloacetamide core would provide hydrophobic interaction with the protease. Therefore, a wide range of functional testing was performed on both aromatic rings in various conformations with the aim of enhancing the pharmacological activity of the compound.

The inhibitory effects of compounds **7a–i** and **8a–e** against DENV2 NS2B/NS3pro were evaluated (Fig. 2) and the results are shown in Table 1. It can be generally inferred from the SAR that the alteration of R^1 contributed to improve the inhibitory activity (e.g. **7c** and **7e**). The substituent in the benzylthio ring influence the inhibitory activity followed the order at F > OCH_3 > Br > Cl. The derivatives with *p*- or *o*-chloro groups displayed similar activity, corresponding to the results for compounds **7f**, and **7i**. An increase the size of the ring in the R^1 part was associated with decreased inhibitory activity, based on the results of compounds **7b** and **7g**. Of note, compound **7a,** which utilized trifluoromethyl to replace benzylthio, retained inhibitory activity against NS2B/NS3pro. Variation of the R^2 group impacted on the inhibitory potency significantly. Both fluorine and nitrile groups in the *p*- and *o*-benzyl group could enhance the inhibitory activity and compounds carrying these groups (**8a**, **8b** and **8e**) displayed strong inhibition of over 85%.

Considering that the strong electro-affinity of the linker part may incur risk of toxicity, another chemical optimization was performed to modify the enamide fragment. This provided the impetus for the synthesis of the denitrile product **12a** and the olefins hydrogenation product **12b**. Surprisingly, both of the compounds were found to be inactive (data not shown), which may suggest an essential role of the enamide part in determining inhibitory activity against NS2B/NS3pro. We speculate that the nitrile group provides a hydrogen bond acceptor that interacts with the protease, and which is therefore crucial to its activity.

The IC_{50} against the DENV NS2B/NS3 protease was determined for those compounds with inhibitory rates over 75%. The results are summarized in Table 2. Six of the synthetic derivatives tested demonstrated significant inhibitory activity, with IC_{50} values of <5 μM. It can be observed that variation of R^2 was a more effective way to improve inhibitory activity than variation of the R^1 groups. Furthermore, small substitutes that can act as a hydrogen bond receptor in the R^2 group (e.g., –F and –CN) produce better results. The most effective compound **8b** (IC_{50} = 2.24 μM) was obtained in this way, which increased the activity by 3 times compared with the lead compound **1** (IC_{50} = 6.09 μM).

To understand the structural basis for the binding affinities of the inhibitors, we scrutinized the 3D binding poses of designed compounds **7a**, **7b**, **8b**, **12a** by molecular docking (Fig. 4A–G). In a preliminary sense, the docking results corroborate the activity trends observed in these four compounds. The key feature in the docked conformation of active compounds (**7a**, **7b**, **8b**) is that the nitrile group is involved in hydrogen-bonding interactions with

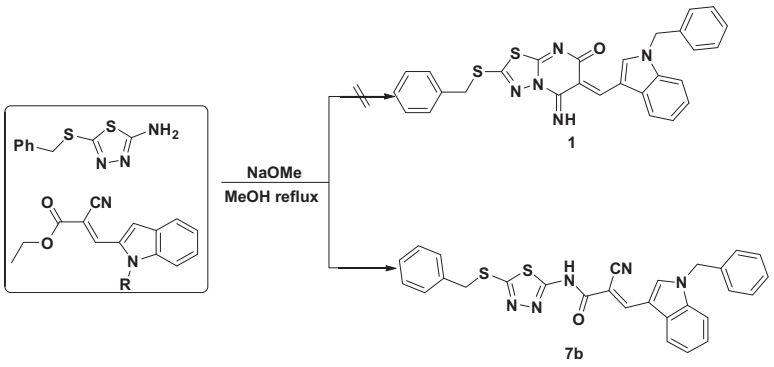

Scheme 1. Results of the cyclization reaction.

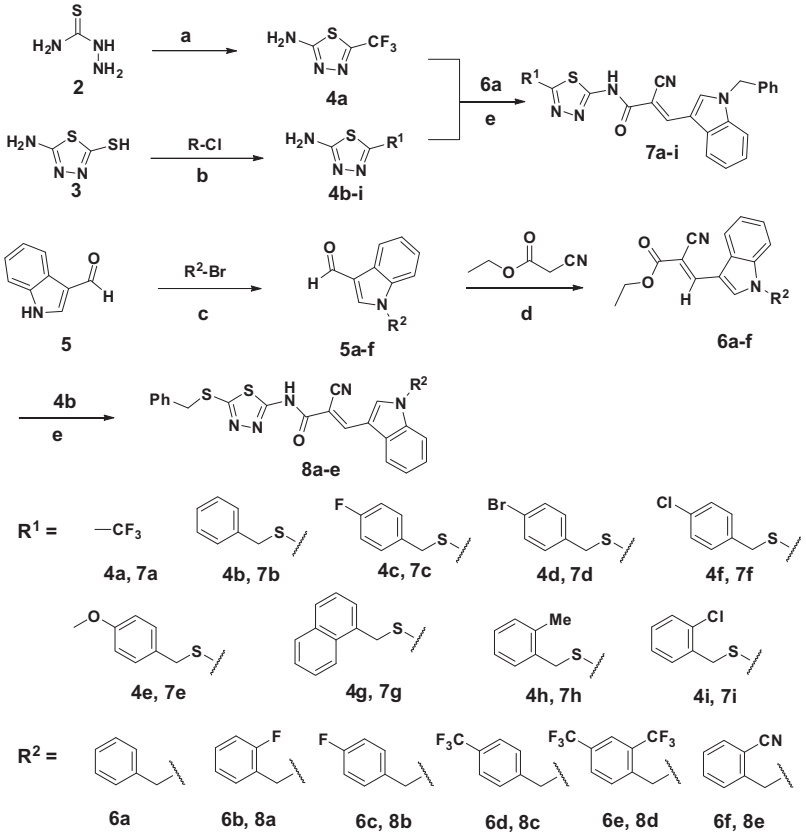

Scheme 2. Reagents and conditions: (a) $(CF_3O)_2O$, 40 °C; (b) MeOH/MeONa, rt; (c) NaH/DMF; (d) Piperidine/EtOH reflux; (e) MeOH/MeONa, reflux.

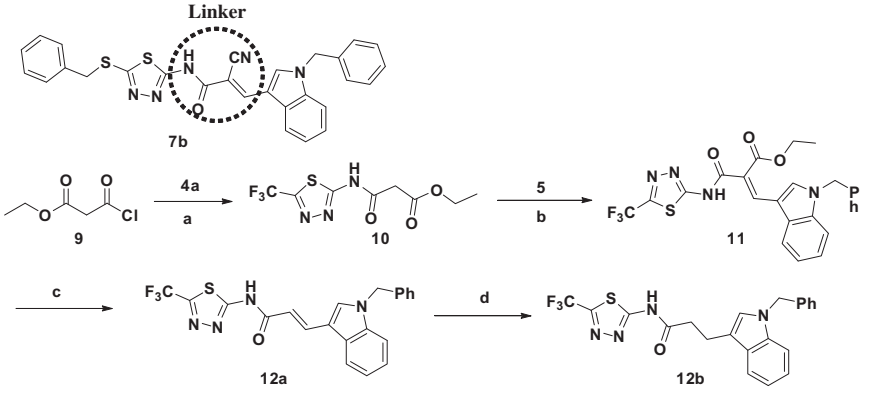

Scheme 3. Reagents and conditions: (a) Et_3N/CH_2Cl_2, 0 °C; (b) Piperidine/EtOH reflux; (c) (1), NaOH/MeOH/H_2O (2), HCl, reflux; (d) H_2/Pd/C, MeOH.

Please cite this article in press as: Liu, H.; et al. *Bioorg. Med. Chem.* (2014), http://dx.doi.org/10.1016/j.bmc.2014.09.057

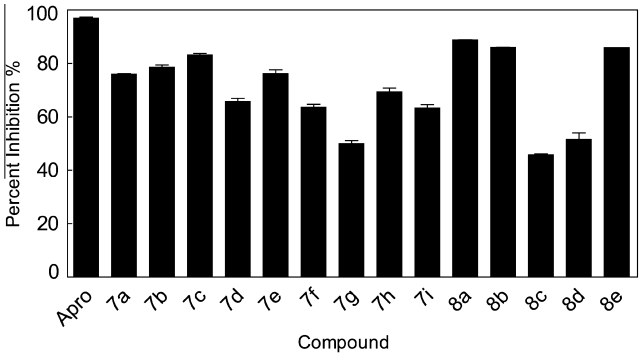

Figure 2. The inhibitory activities of compounds **7a–i** and **8a–e** at 20 μM against DENV2 NS2B/NS3pro. The compounds (20 μM) were incubated with DENV2 NS2B/NS3pro (200 nM) at 37 °C for 30 min, then addition of the substrate (Bz-Nle-Lys-Arg-Arg-AMC, 200 μM) started the reaction. The inhibitory rate was calculated from the relative maximum reaction rate in the presence and absence of tested compound. Every assay was performed in triplicate.

the side chain of Ser83 in pocket S2 and the main chain of Met84. By contrast, the inactive compound **12a** lose these two hydrogen-bonding interactions, supporting an essential role for the nitrile group in determining to the activity of the compound. The benzyl group in the pocket S3 may have hydrophobic interactions with residues, including Val154, Val155, Gly159 and Ile86, which lead to the different binding pattern of **7b** (Fig. 4A) from its non-benzyl counterpart **7a** (Fig. 4C). In addition, the benzyl group in the indole fragment of compound **7b** appears to occupy the pocket S2 better compared with compound **7a** (Fig. 4B and D). These interactions may explain the increase of inhibitory activity observed in benzyl thiol derivatives. The *p*-fluoro in the phenyl group forms H-bonds with the side chain of Arg54 in the S2 region (Fig. 4E), resulting in a better binding affinity with the S2 pocket. This may permit the molecule to bend to the protein more tightly, leading to the enhanced activity of compound **8b**. Next, the binding affinities of **7b** and its analogues, including **7a**, **8b** and **12a**, were also examined by Surface Plasmon Resonance (SPR) technology based Biacore 3000 instrument (GE, Healthcare.). As shown in Fig. 5, **7b** bound to NS2B/NS3 by K_D at 3.59 μM, **7a** at 9.27 μM, and **8b** at 2.07 μM, while **12a** failed to bind to NS2B/NS3. These results were consistent with their enzymatic inhibitory activities against NS2B/NS3 (Fig. 3), further confirming the conclusions from the molecular modeling.

5. Conclusion

In summary, we have demonstrated that the thiadiazoloacetamide core constitutes a novel scaffold upon which DENV NS2B/NS3 protease inhibitors can be developed. Basis on the structure of the initial screening hit, compound **1**, and structural modification was performed and a series of derivatives were synthesized. Most of the products displayed strong inhibitory rates and six were found with IC_{50} <5 μM against the target enzyme. The most potent compound **8b** presented better inhibitory activity than the lead compound **1** (IC_{50} = 2.24 vs 6.09 μM). Furthermore, the performances of docking and binding affinity studies give an insight into the binding modes of these novel compounds. Their combination of potency and synthetic tractability means that the new chemical structures described in this study pave the way for the discovery of small molecule DENV NS2B-NS3 inhibitors.

6. Experimental section

6.1. General

Unless otherwise stated, all reagents used were commercially purchased without further purification. NMR spectra were recorded on Varian-MERCURY Plus-400 in $CDCl_3$ and DMSO-d_6 on a standard spectrometer operating at 400, and 500 MHz (^{1}H 400 MHz, ^{13}C 125 MHz). Infrared spectra were recorded on NICOLET FTIR 6700 spectrophotometer using KBr pellets. Column chromatography was performed with on silica gel (200−300 mesh). TLC was performed on Silica Gel GF254 for TLC and spots were visualized by irradiation with UV light (254 nm). Melting points were measured uncorrected. High-resolution mass spectra were recorded using the EI method on Thermo-DFS. Melting points were measured uncorrected.

6.2. Chemistry

6.2.1. Synthesis of 5-(trifluoromethyl)-1,3,4-thiadiazol-2-amine 4a

A mixture of thiosemicarbazide (2.0 g, 21 mmol), trifluoroacetic acid anhydride (4.6 g, 21 mmol) was stirred at −5 °C for 1 h under nitrogen atmosphere, then reaction mixture was heated at 40 °C overnight. The reaction mixture was poured into ice water (20 mL) and made alkaline with $NaHCO_3$. Then the mixture was filtered, washed with ice water and dried to afford white solid in a yield of 72%. ^{1}H NMR (400 MHz, DMSO-d_6): 7.44 (s, 2H).

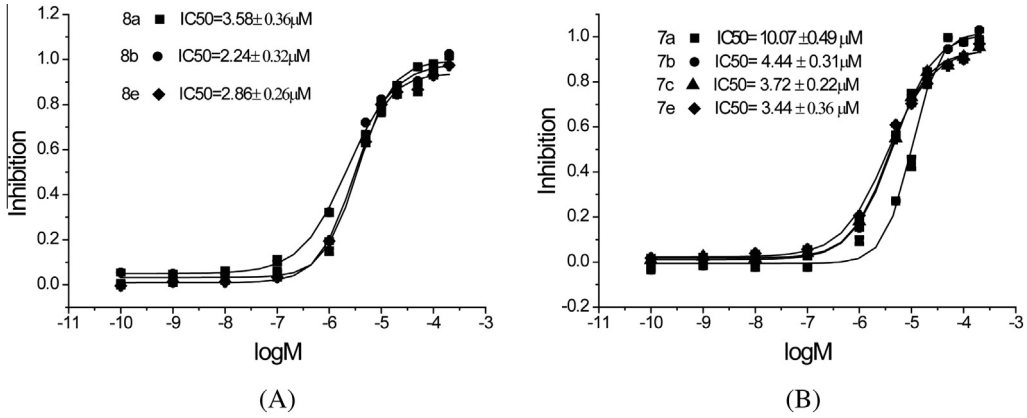

Figure 3. The dose-dependent effects of compounds **7a**, **7b**, **7c**, **7e** (A) and **8a**, **8b**, **8e** (B) against DENV2 NS2B/NS3pro.

Table 1
Structures and percent inhibition against DENV-2 NS2B/NS3 protease

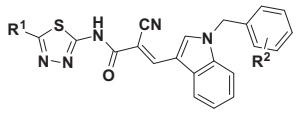

Inhibitor	R^1	R^2	Inhibition rate[a]	Inhibitor	R^1	R^2	Inhibition rate[a]
Apro			97.59 ± 1.4	**7g**	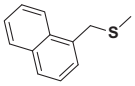	H	50.05 ± 1.6
1			72.01 ± 2.2	**7h**	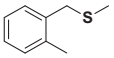	H	69.38 ± 2.1
7a	$-CF_3$	H	76.05 ± 1.1	**7i**	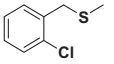	H	63.48 ± 2.2
7b	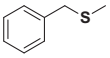	H	78.95 ± 1.9	**8a**	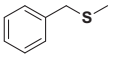	2-F	88.89 ± 0.3
7c	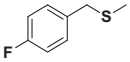	H	83.38 ± 0.9	**8b**	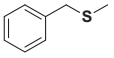	4-F	86.48 ± 1.6
7d	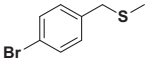	H	65.78 ± 1.5	**8c**	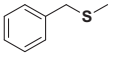	$4-CF_3$	45.87 ± 0.51
7e	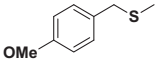	H	76.34 ± 1.4	**8d**	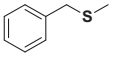	$2,4-CF_3$	54.06 ± 5.5
7f	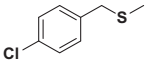	H	63.40 ± 1.8	**8e**	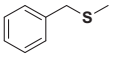	2-CN	85.83 ± 0.7

[a] The inhibition rate was determined as at 20 μM of the tested compounds.

Table 2
IC_{50}values against DENV-2 NS2B/NS3 protease

Inhibitor	IC_{50} (μM)
7a	10.07 ± 0.49
7b	4.44 ± 0.31
7c	3.72 ± 0.22
7e	3.44 ± 0.36
8a	3.58 ± 0.36
8b	2.24 ± 0.32
8e	2.86 ± 0.26

6.2.2. General synthesis of 5-(benzylsulfanyl)-1,3,4-thiadiazol-2-amines 4b–i

To solution of 5-amino-1,3,4-thiadiazole-2-thiol **3** (500 mg, 3.75 mmol) in MeOH (20 mL) was added MeONa (405.6 mg, 7.5 mmol) and stirred. Then benzyl chloro (475 mg, 3.75 mmol) was added to the reaction mixture at room temperature and stirred until a white solid was precipitated. The solid was filtered, washed with methanol to afford **4b** (710 mg, 85%) and it was available for the next reaction. ^{1}H NMR (400 MHz, $CDCl_3$) δ 7.41–7.29 (m, 5H), 5.31 (br, 1H), 4.38 (s, 2H).

6.2.3. General synthesis of 1-benzyl-1*H*-indole-2-carbaldehydes 5a–f

A mixture of 1*H*-indole-2-carbaldehyde **5** (1 g, 8.54 mmol) and NaH (410 mg, 17 mmol) in dry DMF was stirred at 0 °C under nitrogen atmosphere. To this solution was add benzyl bromo (1.46 g, 8.54 mmol). Then the mixture was stirred at room temperature until the reaction was deemed complete by TLC. The reaction mixture was extracted with ethyl acetate (60 mL) and saturated NH_4Cl solution (50 mL × 2), washed with brine (50 mL). After filtration and concentration, the crude mixture obtained was purified by chromatography on silica gel with 4:1 PE/EA mixture as eluent, to give **5a** as a white solid (1.4 g 79%). ^{1}HNMR (400 MHz, $CDCl_3$) δ 5.77 (2H, s), 7.15 (1H, s), 7.10 (1H, s), 7.12–7.23 (4H, m), 7.30 (1H, s), 7.36–7.38 (2H, m), 7.76 (1H, d, *J* = 8.2 Hz), 9.95 (1H, s).

6.2.4. General synthesis of (2*E*)-ethyl-3-(1-benzyl-1*H*-indol-2-yl)-2-cyanoprop-2-enoates 6a–f

To a solution of **5a** (500 mg, 2.13 mmol) in ethanol was add ethylcyanoacetate (240 mg, 2.13 mmol) and three drops of piperidine. The mixture was stirred at 80 °C for 6 h. Then cooled to room temperature and precipitate formed was collected by suction filtration to give **6a** as a yellow solid (632 mg, 90%). ^{1}H NMR (400 MHz, $CDCl_3$) δ 8.64 (d, *J* = 3.7 Hz, 2H), 7.91–7.83 (m, 1H), 7.39–7.30 (m, 6H), 7.22–7.16 (m, 2H), 5.45 (s, 2H), 4.40 (q, *J* = 7.1 Hz, 2H), 1.42 (t, *J* = 7.1 Hz, 3H).

6.2.5. General synthesis of (2*E*)-3-(1-benzyl-1*H*-indol-3-yl)-*N*-(5-(benzylsulfanyl)-1,3,4-thiadiazol-2-yl)-2-cyanoprop-2-enamides 7a–i and 8a–e

To a solution of sodium metal (46 mg, 2 mmol) in dry methanol (15 mL), **4a** (112 mg, 0.5 mmol) and **6a** (165 mg, 0.5 mmol) were added and resulting mixture was refluxed for 2 h. Then cooling the mixture and acidified with acetic acid, the separated yellow solid was collected by filtration and dried to afford the desired products.

6.2.5.1. (*E*)-3-(1-benzyl-1*H*-indol-3-yl)-2-cyano-*N*-(5-(trifluoromethyl)-1,3,4-thiadiazol-2-yl)enamide (7a). Yellow solid (155 mg, 68%), mp >250 °C ^{1}H NMR (400 MHz, $CDCl_3$) δ 9.78 (br, 1H), 8.85 (s, 1H), 8.65 (s, 1H), 7.91 (d, *J* = 8 Hz, 1H), 7.40–7.34 (m, 6H), 7.22–7.20 (m, 2H), 5.47 (s, 2H). HRMS (EI): Calcd for $C_{22}H_{14}F_3N_5OS$ 453.0871; Found 453.0877.

6.2.5.2. (*E*)-3-(1-benzyl-1*H*-indol-3-yl)-*N*-(5-(benzylsulfanyl)-1,3,4-thiadiazol-2-yl)-2-cyanoprop-2-enamide (7b). Yellow solid (146 mg, 73%), mp 207–208 °C. ^{1}H NMR (400 MHz, DMSO) δ 8.84 (s, 1H), 8.69 (s, 1H), 8.09–8.02 (m, 1H), 7.73–7.66 (m, 1H),

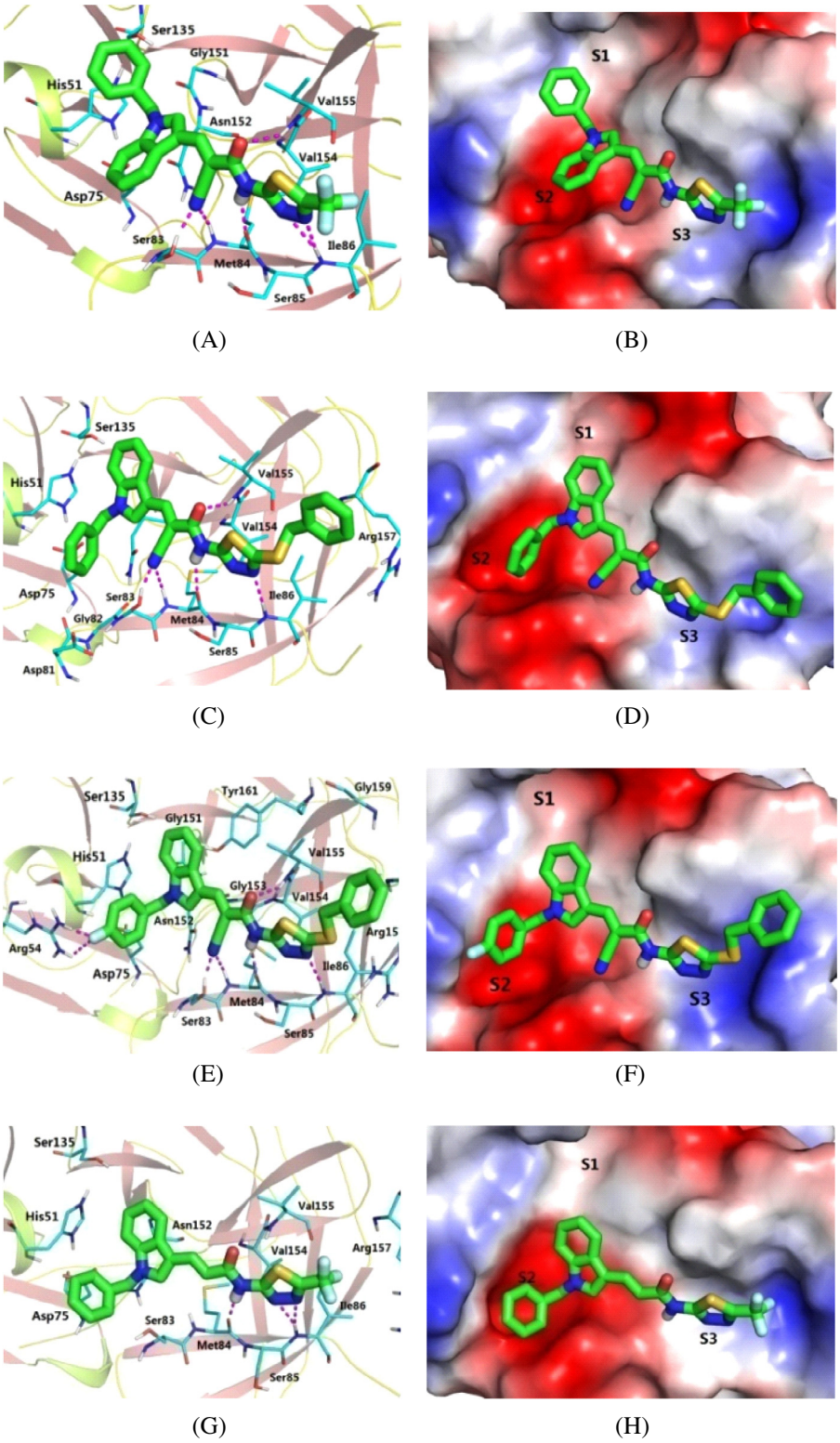

Figure 4. Putative binding mode of selected compounds **7a** (A, B), **7b** (C, D), **8b** (E, F) and **12a** (G, H) interacting with catalytic site of DENV2 NS2B/NS3 protease. The poses were prepared using PyMol (http://pymol.sourceforge.net/). The ligands are shown as sticks, and the non-carbonatoms are colored by atom types. Hydrogen bonds are shown as dotted lines. The NS2B-NS3 surface is colored according to electrostatic potential.

7.44–7.39 (m, 3H), 7.37–7.31 (m, 5H), 7.29–7.25 (m, 2H), 7.20 (t, J = 7.5 Hz, 1H), 5.73 (s, 2H), 4.50 (s, 2H). ^{13}C NMR (125 MHz, DMSO) δ 163.14, 161.20, 144.16, 137.12, 136.47, 134.53, 133.22, 133.20, 130.15, 130.08, 129.50, 129.07, 128.72, 128.11, 124.37, 122.95, 119.57, 116.22, 116.05, 112.30, 110.03. HRMS (EI): Calcd for $C_{28}H_{21}N_5OS_2$ 507.1188; Found 507.1188.

6.2.5.3. (*E*)-3-(1-benzyl-1*H*-indol-3-yl)-2-cyano-*N*-(5-(((4-fluorophenyl)methyl)sulfanyl)-1,3,4-thiadiazol-2-yl)prop-2-enamide (7c). Yellow solid (133 mg, 54%), mp 246–247 °C. ^{1}H NMR (400 MHz, DMSO) δ 8.58 (s, 1H), 8.45 (s, 1H), 7.90–7.88 (m, 1H), 7.73 (d, J = 8.2 Hz, 2H), 7.56–7.54 (m, 1H), 7.44 (d, J = 8.1 Hz, 2H), 7.39–7.37 (m, 2H), 7.34–7.30 (m, 2H), 7.27–7.26 (m, 3H),

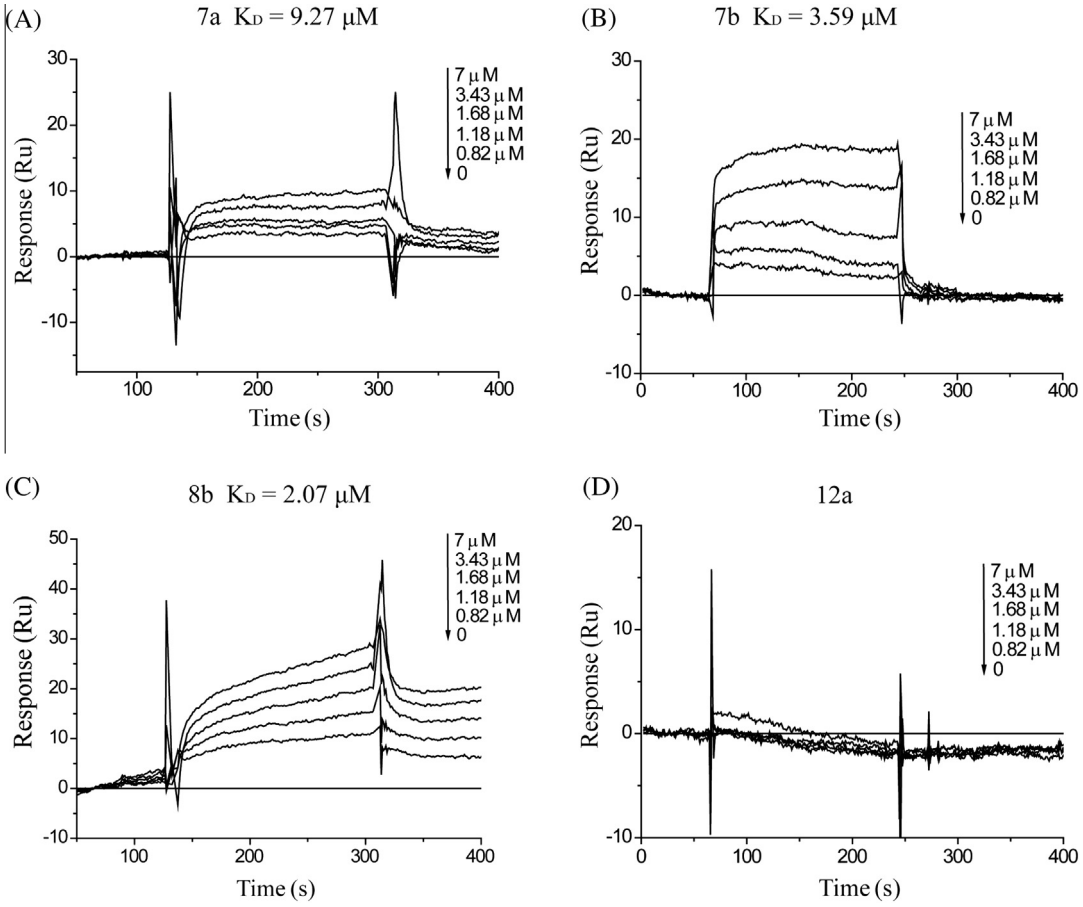

Figure 5. The binding affinities of compounds **7a** (A), **7b** (B), **8b** (C) and **12a** (D) to DENV2 NS2B/NS3pro.

5.76 (s, 2H), 4.36 (s, 2H). HRMS(EI): Calcd for $C_{28}H_{20}FN_5OS_2$ 525.1093; Found 525.1082.

6.2.5.4. (*E*)-3-(1-benzyl-1*H*-indol-3-yl)-*N*-(5-(((4-bromophenyl) methyl)sulfanyl)-1,3,4-thiadiazol-2-yl)-2-cyanoprop-2-enamide (7d). Yellow solid (125 mg, 58%), mp 225–226 °C. ^{1}H NMR (400 MHz, DMSO) δ 8.86 (s, 1H), 8.73 (s, 1H), 8.10–8.03 (m, 1H), 7.68–7.62 (m, 1H), 7.57–7.52 (m, 2H), 7.40–7.29 (m, 9H), 5.68 (s, 2H), 4.49 (s, 2H). HRMS (EI): Calcd for $C_{28}H_{20}BrN_5OS_2$ 585.0293; Found 585.0300.

6.2.5.5. (*E*)-3-(1-benzyl-1*H*-indol-3-yl)-2-cyano-*N*-(5-(((4-methoxyphenyl)methyl)sulfanyl)-1,3,4-thiadiazol-2-yl)prop-2-enamide (7e). Yellow solid (152 mg, 50%), mp 213–215 °C. ^{1}H NMR (400 MHz, DMSO) δ 8.86 (s, 1H), 8.73 (s, 1H), 8.11–8.04 (m, 1H), 7.66–7.63 (m, 1H), 7.38–7.29 (m, 9H), 6.92–6.88 (m, 2H), 5.68 (s, 2H), 4.46 (s, 2H), 3.74 (s, 3H). HRMS (EI): Calcd for $C_{22}H_{14}N_5O_2S_2$ 537.1293; Found 537.1303.

6.2.5.6. (*E*)-3-(1-benzyl-1*H*-indol-3-yl)-*N*-(5-(((4-chlorophenyl)-methyl)sulfanyl)-1,3,4-thiadiazol-2-yl)-2-cyanoprop-2-enamide (7f). Yellow solid (102 mg, 70%), mp 221–222 °C. ^{1}H NMR (400 MHz, DMSO) δ 8.87 (s, 1H), 8.73 (s, 1H), 8.12–8.03 (m, 1H), 7.69–7.63 (m, 1H), 7.48–7.29 (m, 11H), 5.68 (s, 2H), 4.51 (s, 2H). HRMS (EI): Calcd for $C_{28}H_{20}ClN_5OS_2$ 541.0798; Found 541.0807.

6.2.5.7. (*E*)-3-(1-benzyl-1*H*-indol-3-yl)-2-cyano-*N*-(5-((naphthalen-1-ylmethyl)sulfanyl)-1,3,4-thiadiazol-2-yl)prop-2-enamide (7g). Yellow solid (115 mg, 63%), mp 198–200 °C.^{1}H NMR (400 MHz, DMSO) δ 8.72 (s, 1H), 8.67 (s, 1H), 8.22 (d, J = 8.5 Hz, 1H), 8.03–7.96 (m, 2H), 7.89 (d, J = 8.2 Hz, 1H), 7.65–7.54 (m, 4H), 7.46–7.42 (m, 1H), 7.39–7.27 (m, 7H), 5.66 (s, 2H), 4.95 (s, 2H). HRMS (EI): Calcd for $C_{32}H_{23}N_5OS_2$ 547.1344; Found 557.1326.

6.2.5.8. (*E*)-3-(1-benzyl-1*H*-indol-3-yl)-2-cyano-*N*-(5-(((2-methylphen-yl)methyl)sulfanyl)-1,3,4-thiadiazol-2-yl)prop-2-enamide (7h). Yellow solid (107 mg, 65%), mp 216–218 °C. ^{1}H NMR (400 MHz, DMSO) δ 8.82 (s, 1H), 8.71 (s, 1H), 8.08–8.01 (m, 1H), 7.67–7.62 (m, 1H), 7.39–7.28 (m, 8H), 7.24–7.19 (m, 2H), 7.18–7.13 (m, 1H), 5.68 (s, 2H), 4.50 (s, 2H), 2.39 (s, 3H). HRMS (EI): Calcd for $C_{29}H_{23}N_5OS_2$ 521.1344; Found 521.1342.

6.2.5.9. (*E*)-3-(1-benzyl-1*H*-indol-3-yl)-*N*-(5-(((2-chlorophenyl)-methyl)sulfanyl)-1,3,4-thiadiazol-2-yl)-2-cyanoprop-2-enamide (7i). Yellow solid (107 mg, 53%), mp 210–211 °C. ^{1}H NMR (400 MHz, DMSO) δ 8.88 (s, 1H), 8.74 (s, 1H), 8.12–8.04 (m, 1H), 7.70–7.62 (m, 1H), 7.52 (td, J = 7.2, 1.8 Hz, 2H), 7.39–7.29 (m, 9H), 5.69 (s, 2H), 4.58 (s, 2H). HRMS (EI): Calcd for $C_{28}H_{20}ClN_5OS_2$ 541.0798; Found 541.0803.

6.2.5.10. (*E*)-*N*-(5-(benzylsulfanyl)-1,3,4-thiadiazol-2-yl)-2-cyano-3-(1-((2-fluorophenyl)methyl)-1*H*-indol-3-yl)prop-2-enamide (8a). Yellow solid (121 mg, 65%), mp 201–202 °C. ^{1}H NMR (400 MHz, DMSO) δ 8.84 (s, 1H), 8.69 (s, 1H), 8.09–8.01 (m, 1H), 7.73–7.66 (m, 1H), 7.44–7.38 (m, 3H), 7.37–7.32 (m, 5H), 7.30–7.24 (m, 2H), 7.20 (t, J = 7.5 Hz, 1H), 5.73 (s, 2H), 4.50 (s, 2H). HRMS (EI): Calcd for $C_{28}H_{20}FN_5OS_2$ 525.1093; Found 525.1084.

6.2.5.11. (*E*)-*N*-(5-(benzylsulfanyl)-1,3,4-thiadiazol-2-yl)-2-cyano-3-(1-((4-fluorophenyl)methyl)-1*H*-indol-3-yl)prop-2-enamide (8b). Yellow solid (127 mg, 48%), mp 219–220 °C. ^{1}H NMR (400 MHz, DMSO) δ 8.86 (s, 1H), 8.73 (s, 1H), 8.06 (br, 1H), 7.71–7.63 (m, 1H), 7.45–7.42 (m, 2H), 7.41–7.32 (m, 6H), 7.31–7.27 (m, 1H), 7.23–7.17 (m, 2H), 5.66 (s, 2H), 4.50 (s, 2H). HRMS (EI): Calcd for $C_{28}H_{20}FN_5OS_2$ 525.1093; Found 525.1092.

6.2.5.12. (*E*)-*N*-(5-(benzylsulfanyl)-1,3,4-thiadiazol-2-yl)-2-cyano-3-(1-((4-(trifluoromethyl)phenyl)methyl)-1*H*-indol-3-yl)prop-2-enamide (8c). Yellow solid (130 mg, 70%), mp 218–220 °C. ^{1}H NMR (400 MHz, DMSO) δ 8.58 (s, 1H), 8.45 (s, 1H), 7.90–7.88 (m, 1H), 7.73 (d, J = 8.2 Hz, 2H), 7.56–7.54 (m, 1H), 7.44 (d, J = 8.1 Hz, 2H), 7.39–7.37 (m, 2H), 7.34–7.30 (m, 2H), 7.27–7.24 (m, 3H), 5.76 (s, 2H), 4.37 (s, 2H). HRMS (EI): Calcd for $C_{29}H_{20}F_3N_5OS_2$ 575.1061; Found 575.1058.

6.2.5.13. (*E*)-*N*-(5-(benzylsulfanyl)-1,3,4-thiadiazol-2-yl)-3-(1-((2,4-bis(tri-fluoromethyl)phenyl)methyl)-1*H*-indol-3-yl)-2-cyanoprop-2-enamide (8d). Yellow solid (107 mg, 69%), mp 226–227 °C. ^{1}H NMR (400 MHz, DMSO) δ 8.80–8.79 (m, 2H), 8.09–8.04 (m, 4H), 7.70–7.69 (m, 1H), 7.43–7.41 (m, 2H), 7.36–7.27 (m, 5H), 5.88 (s, 2H), 4.49 (s, 2H). HRMS (EI): Calcd for $C_{30}H_{19}F_6N_5OS_2$ 643.1035; Found 643.0933.

6.2.5.14. (*E*)-*N*-(5-(benzylsulfanyl)-1,3,4-thiadiazol-2-yl)-2-cyano-3-(1-((2-cyanophenyl)methyl)-1*H*-indol-3-yl)prop-2-enamide (8e). Yellow solid (140 mg, 70%), mp 224–226 °C. ^{1}H NMR (400 MHz, DMSO) δ 8.87 (s, 1H), 8.71 (s, 1H), 8.11 (d, J = 8 Hz, 1H), 7.95 (d, J = 7.3 Hz, 1H), 7.66 (t, J = 7.7 Hz, 1H), 7.60 (d, J = 7.1 Hz, 1H), 7.54 (t, J = 7.4 Hz, 1H), 7.43 - 7.42(m, 2H), 7.36–7.29 (m, 5H), 7.07 (d, J = 8.2 Hz, 1H), 5.93 (s, 2H), 4.51 (s, 2H). HRMS (EI): Calcd for $C_{29}H_{20}N_6OS_2$ 532.1140; Found 532.1120.

6.2.6. Synthesis of ethyl-2-((5-(trifluoromethyl)-1,3,4-thiadiazol-2-yl)carbamoyl)acetate 10

A solution of **4a** (1 g, 4.14 mmol) in dry DCM was stirred at 0 °C under nitrogen atmosphere, then ethyl malonyl chloride (686 mg, 4.56 mmol) was slowly dropped to the solution. Then 0.5 mL of triethylamine was added to the mixture and the mixture was stirred at room temperature until the reaction was deemed complete by TLC. The reaction mixture was extracted with DCM (60 mL) and saturated $NaHCO_3$ solution (50 mL × 2), washed with brine (50 mL). After filtration and concentration, the crude mixture obtained was purified by chromatography on silica gel with 4:1 PE/EA mixture as eluent, to give **10** as white solid (860 mg, 59%). ^{1}H NMR (400 MHz, $CDCl_3$) δ 12.63 (s, 1H), 4.30 (q, J = 7.1 Hz, 2H), 3.79 (s, 2H), 1.34 (t, J = 7.1 Hz, 3H).

6.2.7. Synthesis of ethyl (*E*)-3-(1-benzyl-1*H*-indol-2-yl)-2-((5-(trifluoromethyl)-1,3,4-thiadiazol-2-yl)carbamoyl)prop-2-enoate 11

The enoate **11** was synthesized using the way similar with **6a**. Yellow solid (370 mg, 87%).^{1}H NMR (400 MHz, $CDCl_3$) δ 12.87 (s, 1H), 9.38 (s, 1H), 8.95 (s, 1H), 7.89 (d, J = 7.8 Hz, 1H), 7.42–7.30 (m, 6H), 7.23 (d, J = 6.8 Hz, 2H), 5.52 (s, 2H), 4.47 (q, J = 7.2 Hz, 2H), 1.51 (t, J = 7.1 Hz, 3H).

6.2.8. Synthesis of (*E*)-3-(1-benzyl-1*H*-indol-2-yl)-2-formyl-*N*-(5-(trifluoromethyl)-1,3,4-thiadiazol-2-yl)prop-2-enamide 12a

A mixture of **11** (300 mg, 0.594 mmol) in MeOH/H_2O (1:2 v/v) was added 5 M aqueous NaOH (1 mL) and stirred at room temperature for 4 h. Then the mixture was acidified with concentrated HCl and heated to 120 °C. After the conversion was complete, the mixture was extracted with EA (50 mL × 2). The combined organic layers were washed brine and dried over anhydrous $MgSO_4$. After removal of solvent, the oily crude product was purified by chromatography with 40:1 $CHCl_2$/MeOH mixture as eluent to afford **12a** as a white solid (160 mg, 60%). mp 202–203 °C. ^{1}H NMR (400 MHz, DMSO) δ 12.86 (br, 1H), 8.14 (s, 1H), 7.97–7.89 (m, 2H), 7.58–7.57 (m, 1H), 7.33–7.31 (m, 2H), 7.28–7.20 (m, 5H), 6.88 (d, J = 16.0 Hz, 1H), 5.49 (s, 2H). ^{13}C NMR (125 MHz, DMSO) δ 178.06, 137.75, 135.66, 129.14, 128.10, 127.65, 126.06, 123.31, 121.83, 120.65, 112.34, 111.88. HRMS (EI): Calcd for $C_{21}H_{15}F_3N_4OS$ 428.0919; Found 428.0952.

6.2.9. Synthesis of (*E*)-3-(1-benzyl-1*H*-indol-2-yl)-*N*-(5-(trifluoromethy-l)-1,3,4-thiadiazol- 2-yl)prop-2-enamide 12b

To a solution of **12a** (100 mg, 0.224 mmol) in MeOH was added Pt/C. The mixture was stirred at room temperature hydrogen under atmosphere for 24 h. Then the mixture was filtered and the organic layer was concentrated. The oily crude product was purified by chromatography with 20:1 $CHCl_2$/MeOH mixture as eluent to afford **12b** as a white solid (48 mg, 47%), mp 202–203 °C. ^{1}H NMR (400 MHz, DMSO) δ 13.26 (br, 1H), 7.59 (d, J = 7.8 Hz, 1H), 7.39 (d, J = 8.1 Hz, 1H), 7.25 (s, 1H), 7.20–7.15 (m, 3H), 7.14–7.04 (m, 3H), 7.01 (t, J = 7.0 Hz, 1H), 5.33 (s, 2H), 3.09 (t, J = 7.3 Hz, 2H), 2.93 (t, J = 7.3 Hz, 2H). HRMS (EI): Calcd for $C_{21}H_{17}F_3N_4OS$ 430.1075; Found 430.1067.

6.3. Biochemistry

6.3.1. DENV2 NS2B/NS3pro expression and purification

The plasmid of pET15b-DEN2 containing CF40-Gly-NS3pro185 was donated from Prof. Chunguang Wang (Institute of Protein Research, Tongji University). The plasmid was transformed into *Escherichia coli* BL21, and then DENV2 NS2B-NS3 expression and purification was performed as previously described.[28]

6.3.2. In vitro DENV2 NS2B/NS3pro assays and inhibition studies

Protease assay was carried out in Greiner Black 96 well plates. Each assay consisted of the reaction mixture of 100 μL containing 50 mM Tris-HCl, pH 8.5, 10 mM NaCl, 20% v/v glycerol, 1 mM CHAPS, 200nM DENV2 NS2B-NS3 pro and 20 μM tested compound. The concentration of positive inhibitor (*Aprotinin*) was 1 μM. The compounds were dissolved in dimethylsulfoxide (DMSO) and the final DMSO concentration in the assay was 1% v/v. The enzyme and the compound were pre-incubated at 37 °C for 30 min, and then the substrate (Bz-Nle-Lys-Arg-Arg-AMC, 200 μM) was added to initiate the reaction. The fluorescence was continuously monitored every 10s for 5 min with a spectrofluorometer (SpectraMax M5) at 380 nm excitation/460 nm emission.

For determining IC_{50} values, the tested compound in eleven concentrations (0.1, 1, 10, 100 nM, 1, 5, 10, 20, 50, 100, 200 μM) were mixed with enzyme in the assay buffer. IC_{50} values were calculated using the OriginPro 8. Every assay was performed in triplicate.

6.3.3. SPR-based ligand binding assay

The equilibrium dissociation constant (K_D) of the compound binding to DENV2 NS2B/NS3pro was detected by Biacore 3000 based on SPR technology. Briefly, purified DENV2 NS2B/NS3pro was immobilized onto CM5 sensor chip by standard amine-coupling procedure in 10 mM sodium acetate buffer (pH 3.95). Compounds were then serially diluted by HBS buffer (0.01 M HEPES, 0.15 M NaCl, 3 mM EDTA, pH 7.4, 0.005% surfactant P20) and injected into the channels at a flow rate of 30 μL/min for 180 s, followed by dissociation for 240 s. BIAevaluation software (version 3.1; Biacore) was used to determine the equilibrium dissociation constant (K_D) of the compounds against the protein.

6.4. Molecular modeling

In this study, we use the crystal structure of DENV3 NS2B-NS3pro structure (PDB ID: 3U1I[29]) with resolution of 2.3 Å as the template to model the structure of DENV2 NS2B-NS3pro. The structure is modeled for molecular docking with the homology software MODELLER 9.12 and analyzed by PROCHECK. From Ramachandran plots, more than 91% of residues of the homology models are located in the most favoured regions and no residue is detected in the disallowed regions. We used maestro to perform the docking studies. In order to know the SAR of the compounds, the compounds are docked according to the IFD protocol developed by Schrödinger (Schrödinger LLC).[30,31]

Acknowledgments

We gratefully acknowledge financial support from the National Natural Science Foundation of China (Grants 81220108025, 21021063, 91229204, and 81025017), National S&T Major Projects (2012ZX09103101-072, 2012ZX09301001-005, and 2013ZX09507-001), Program of Shanghai Subject Chief Scientist (Grant 12XD1407100) and Silver Project (260644).

Supplementary data

Supplementary data associated with this article can be found, in the online version, at http://dx.doi.org/10.1016/j.bmc.2014.09.057.

References and notes

1. Chua, J. E.; Ng, M. L.; Chow, T. K. *Virus Res.* **2004**, *102*, 151.
2. Murgue, B. *Microbes Infect.* **2010**, *12*, 113.
3. Noble, C. G.; Chen, Y. L.; Dong, H.; Gu, F.; Lim, S. P.; Schul, W.; Wang, Q. Y.; Shi, P. Y. *Antiviral Res.* **2010**, *85*, 450.
4. Chaturvedi, U. C.; Shrivastava, R.; Nagar, R. *Indian J. Med. Res.* **2005**, *121*, 639.
5. Irie, K.; Mohan, P. M.; Sasaguri, Y.; Putnak, R.; Padmanabhan, R. *Gene* **1989**, *75*, 197.
6. Chambers, T. J.; Hahn, C. S.; Galler, R.; Rice, C. M. *Annu. Rev. Microbiol.* **1990**, *44*, 649.
7. Bazan, J. F.; Fletterick, R. J. *Virology* **1989**, *171*, 637.
8. Sampatha, A.; Padmanabhan, R. *Antiviral Res.* **2009**, *81*, 6.
9. Yusof, R.; Clum, S.; Wetzel, M.; Murthy, H. M.; Padmanabhan, R. *J. Biol. Chem.* **2000**, *275*, 9963.
10. Schuller, A.; Yin, Z.; Chia, B. C. S.; Doan, D. N. P.; Kim, H.-K.; Shang, L.; Loh, T. P.; Hill, J.; Vasudevan, S. G. *Antiviral Res.* **2011**, *92*, 96.
11. Yin, Z.; Patel, S. J.; Wang, W. L.; Chan, W. L.; RangaRao, K. R.; Ngew, X.; Patel, V.; Beer, D.; Knox, J. E.; Ma, N. L.; Ehrhardt, C.; Lim, S. P.; Vasudevan, S. G.; Keller, T. H. *Bioorg. Med. Chem. Lett.* **2006**, *16*, 40.
12. Knox, J. E.; Ma, N. L.; Yin, Z.; Patel, S. J.; Wang, W. L.; Wang, G.; Chan, W. L.; Vanga Rao, K. R.; Wang, G.; Ngew, X.; Patel, V.; Beer, D.; Lim, S. P.; Vasudevan, S. G.; Keller, T. H. *J. Med. Chem.* **2006**, *49*, 6585.
13. Yin, Z.; Patel, S. J.; Wang, W. L.; Wang, G.; Chan, W. L.; Rao, K. R.; Alam, J.; Jeyaraj, D. A.; Ngew, X.; Patel, V.; Beer, D.; Lim, S. P.; Vasudevan, S. G.; Keller, T. H. *Bioorg. Med. Chem. Lett.* **2006**, *16*, 36.
14. Gao, Y.; Cui, T.; Lam, Y. *Bioorg. Med. Chem.* **2010**, *18*, 1331.
15. Xu, S. Q.; Li, H.; Shao, X. X.; Fan, C. X.; Ericksen, B.; Liu, J. S.; Chi, C. W.; Wang, C. G. *J. Med. Chem.* **2012**, *55*, 6881.
16. Nitsche, C.; Behnam, M. A. M.; Steuer, C.; Klein, C. D. *Antiviral Res.* **2012**, *94*, 72.
17. Tomlinson, S. M.; Watowich, S. J. *Antiviral Res.* **2011**, *89*, 127.
18. Aravapalli, S.; Lai, H.; Teramoto, T.; Alliston, K. R.; Lushington, G. H.; Ferguson, E. L.; Padmanabhan, R.; Groutas, W. C. *Bioorg. Med. Chem.* **2012**, *20*, 4140.
19. Christoph, N.; Christian, S.; Christian, D. K. *Bioorg. Med. Chem.* **2011**, *19*, 7318.
20. Tiew, K. C.; Dou, D.; Teramoto, T.; Lai, H.; Alliston, K. R.; Lushington, G. H.; Padmanabhan, R.; Groutas, W. C. *Bioorg. Med. Chem.* **2012**, *20*, 1213.
21. Lai, H.; Dou, D.; Aravapalli, S.; Teramoto, T.; Lushington, G. H.; Mwania, T. M.; Alliston, K. R.; Eichhorn, D. M.; Padmanabhan, R.; Groutas, W. *Bioorg. Med. Chem.* **2013**, *21*, 102.
22. Knehans, T.; Schüller, A.; Doan, D. N.; Nacro, K.; Hill, J.; Güntert, P.; Madhusudhan, M. S.; Weil, T.; Vasude van, S. G *J. Comput.-Aided. Mol. Des.* **2011**, *25*, 263.
23. Frimayanti, N.; Chee, C.; Zain, S. M.; Rahman, N. A. *Int. J. Mol. Sci.* **2011**, *1089*, 12.
24. Santagati, A.; Santagati, M.; Russo, F.; Ronsisvalle, G. *J. Heterocycl. Chem.* **1988**, *25*, 949.
25. Tsuji, T. *J. Heterocycl. Chem.* **1991**, *28*, 489.
26. Alegaon, S. G.; Alagawadi, K. R.; Sonkusare, P. V.; Chaudhary, S. M.; Dadwe, D. H.; Shah, A. S. *Bioorg. Med. Chem. Lett.* **1917**, *2012*, 22.
27. De, S. K.; Stebbins, J. L.; Chen, L.; Riel-mehan, M.; Machleidt, T.; Dahl, R.; Yuan, H.; Emdadi, A.; Barile, E.; Chen, V.; Murphy, R.; Pellecchia, M. *J. Med. Chem.* **1943**, *2009*, 52.
28. Li, J.; Lim, S. P.; Beer, D.; Patel, V.; Wen, D.; Tumanut, C.; Tully, D. C.; Williams, J. A.; Jiricek, J.; Priestle, J. P.; Harris, J. L. *J. Biol. Chem.* **2005**, *280*, 28766.
29. Noble, C. G.; She, C. C.; Chao, A. T.; Shi, P.-Y. *J. Virol.* **2012**, *86*, 438.
30. Sherman, W.; Day, T.; Jacobson, M. P.; Friesner, R. A.; Farid, R. *J. Med. Chem.* **2006**, *49*, 534.
31. Sherman, W.; Beard, H. S.; Farid, R. *Chem. Biol. Drug Des.* **2006**, *67*, 83.